



**HAL**  
open science

## Study of interval infrared Airflow Drying: A case study of butternut (*Cucurbita moschata*)

Colette Besombes, Chaima Rekik, Collette Besombes, Wafa Hajji, Hela Gliguem, Sihem Bellagha, Arun Mujumdar, Karim Allaf

### ► To cite this version:

Colette Besombes, Chaima Rekik, Collette Besombes, Wafa Hajji, Hela Gliguem, et al.. Study of interval infrared Airflow Drying: A case study of butternut (*Cucurbita moschata*). *LWT - Food Science and Technology*, 2021, 147, pp.111486. 10.1016/j.lwt.2021.111486 . hal-03429644

HAL Id: hal-03429644

<https://univ-rochelle.hal.science/hal-03429644>

Submitted on 9 May 2023

**HAL** is a multi-disciplinary open access archive for the deposit and dissemination of scientific research documents, whether they are published or not. The documents may come from teaching and research institutions in France or abroad, or from public or private research centers.

L'archive ouverte pluridisciplinaire **HAL**, est destinée au dépôt et à la diffusion de documents scientifiques de niveau recherche, publiés ou non, émanant des établissements d'enseignement et de recherche français ou étrangers, des laboratoires publics ou privés.



Distributed under a Creative Commons Attribution - NonCommercial 4.0 International License

1 **Study of Interval Infrared Airflow Drying: a case study of butter-**  
2 **nut (*Cucurbita moschata*)**

3 Chaima Rekik<sup>a</sup>, Collette Besombes<sup>b</sup>, Wafa Hajji<sup>a</sup>, Hela Gliguem<sup>a</sup>, Sihem Bel-  
4 lagha<sup>a</sup>, Arun S Mujumdar<sup>c</sup>, Karim Allaf<sup>b</sup>

5 <sup>a</sup> Research Unit PATIO (UR17AGR01): Promoting Tunisian Natural and Agri-Food Heritage  
6 through Innovation, National Institute of Agronomy of Tunisia, University of Carthage, Tunis  
7 Mahrajene, Tunis

8 <sup>b</sup> Laboratory of Engineering Science for Environment (LaSIE), University of La Rochelle, La  
9 Rochelle, France

10 <sup>c</sup> Department of Bioresource Engineering, Macdonald Campus, McGill University, Montreal,  
11 Quebec, Canada

12

13

14 Corresponding author: Prof. Karim Allaf

15 kallaf@univ-lr.fr

16

## 17 **Abstract**

18 Interval process is defined as a means of operating short-time intervals configured to allow  
19 the material to attain characteristics to match higher drying rate. The innovative Interval  
20 Infra-Red Airflow Drying (IIRAD) involves successive heating intervals ( $t_{ON}$ ) of several  
21 seconds followed by tempering periods ( $t_{OFF}$ ) of a few minutes. IIRAD provides heat only  
22 when the product surface is fully rewetted. Drying of winter squash slices was performed  
23 in three cases; continuous IR-drying, IIRAD-I:  $t_{ON}=5$  s and  $t_{OFF}=2$  min, and IIRAD-II:  $t_{ON}$   
24 varies throughout the process with  $t_{OFF}=2$  min. A higher drying rate was observed during  
25 IIRAD-I. Measured evaporating-bulb temperatures were below  $21^{\circ}\text{C}$  with energy  
26 consumption of 0.98 and 0.77 kWh/kg of evaporated water for I-IIRAD and II-IIRAD,  
27 respectively, wherein they exceeded  $66^{\circ}\text{C}$  and 2.19 kWh/kg of evaporated water for  
28 continuous drying. IIRAD resulted in better preservation of flavonoids and better retention  
29 of color. However, continuous IR-dried samples displayed better rehydration and higher  
30 total polyphenol content. Overall, IIRAD is shown to be a promising drying technique for  
31 heat sensitive materials in terms of efficiency, energy consumption, and preservation of key  
32 quality attributes linked to lower operating temperature, but with increased drying time.

## 33 **Keywords:**

34 IIRAD drying; interval process; energy consumption; quality

35

## 36 **1. Introduction**

37 Interval process may be defined broadly as a way of performing a transformation, operation or  
38 reaction at specified intervals, specially configured to allow the material to attain  
39 characteristics that allow it to be optimally suited to the desired active process. Hence, the  
40 interval process consists of stopping the main treatment or adopting a specific action aimed at  
41 delivering the material in the best state for the main process. Thus, when shrinkage or collapse  
42 reduce the diffusivity of water within the material, the drying rate may be maintained or  
43 strengthened thanks to a texturing interval causing controlled expansion, better diffusivity  
44 and/or increased tortuosity. Thus, the interval of Instant Controlled Pressure-Drop DIC  
45 operation leads to an improvement in the material characteristics making it much more  
46 suitable for drying (Allaf and Allaf, 2014; Mounir, Besombes, Al-Bitar, & Allaf, 2011; Téllez-  
47 Pérez et al., 2012).

48 Other interval drying processes can be defined in close connection with the drying operations.  
49 Regardless of the procedure considered, drying consists of evaporation of water from the  
50 exchange surface and transfer of water from the matrix core toward the surface. The classic  
51 drying operation is controlled by the coupling between these two mechanisms. Interval drying  
52 has been defined as successive independent intervals of water evaporation and mass transfer  
53 (Hajji, Bellagha, & Allaf, 2020). The definition of these intervals and their durations and  
54 evolutions needs to be derived from phenomenological studies including the mechanisms and  
55 structural as well as functional assessments. Interval drying conditions i.e., active and  
56 tempering times should be set in accordance with the product characteristics in order to reach  
57 better drying energy performance and dried product quality.

58 Winter squash “butternut types” (*Cucurbita moschata*) is a good source of fiber, vitamin C,  
59 minerals (calcium, iron, phosphorus), phenolic compounds and pro-vitamin A in the form of

60 total carotenoids. It is a low-fat content product with 126-167 kJ/100g (Armesto et al., 2020).  
61 However, squash is a highly hydrated fruit with 85-94% moisture content (Armesto et al.,  
62 2020; Zaccari & Galietta, 2015), which makes it highly perishable and subject to microbial  
63 deterioration. Drying allows preserving it with extended shelf-life.

64 Although convective drying is the most employed cost-effective drying technique used in  
65 85% of industrial drying operations (Moses, Norton, Alagusundaram, & Tiwari, 2014), it  
66 requires long drying time, high energy consumption, and may yield low final quality. Indeed,  
67 the long drying time and possibly high temperature can lead to degradation of the product  
68 quality in terms of nutritional, functional, and sensorial attributes and also casehardening of  
69 the product (Onwude, Hashim, Abdan, Janius, & Chen, 2019; Pawar & Pratape, 2017; Samadi  
70 & Loghmanieh, 2013; Sui, Yang, Ye, Li, & Wang, 2014). The use of low temperature drying  
71 reduces this degradation but promotes mold and fungi growth. Infrared (IR) drying of  
72 foodstuff was proposed as a good inexpensive and easy to install alternative. However, on an  
73 industrial scale, it is currently used in the dehydration of non-foods, very thin materials such  
74 as coated films and strips (Ratti & Mujumdar, 2006). Nevertheless, the number of research  
75 studies on infrared drying of foodstuff is increasing considerably (Doymaz, Kipcak, & Piskin,  
76 2016; Kayran & Doymaz, 2017; Samadi & Loghmanieh, 2013; Shi et al., 2008; Umesh  
77 Hebbar & Rastogi, 2001), possibly combined to other drying methods (Beigi, 2017;  
78 Dongbang & Matthujak, 2013; Fernando, Low, & Ahmad, 2011; Hebbar, Vishwanathan, &  
79 Ramesh, 2004; Wanyo, Siriamornpun, & Meeso, 2011).

80 Infrared radiation can improve drying rate and lower energy consumption (Ismail, 2016) by  
81 up to 82-86% compared to convective drying (Samadi & Loghmanieh, 2013). Combined both  
82 infrared and vapor convective drying can enhance drying rate and save energy. However,  
83 these two combined heat sources can also overheat the sample and decrease its quality  
84 (Vishwanathan, Hebbar, & Raghavarao, 2010).

85 To alleviate these potential problems, some researchers have proposed intermittency or  
86 sequential infrared and convective drying (Onwude et al., 2019; Sui et al., 2014). Indeed, two  
87 physical mechanisms take place during the drying of a product: (i) generation of vapor, which  
88 has to be transported from the surface to the surrounding air medium, and (ii) a water  
89 diffusion within the solid matrix towards its surface. During conventional drying modes, these  
90 two coupled mechanisms allow control of the operation by limiting these processes. The  
91 external drying conditions of airflow temperature, velocity, and humidity, as well as IR  
92 power-density and types are easily controllable. Thus, the internal water diffusion depends on  
93 the structure of the material and, in the case of foodstuffs and especially plant-origin  
94 materials, the compactness and low permeability of the cell-walls mean that water diffusion is  
95 so low that it becomes the limiting phenomenon during the drying process. Once the amount  
96 of water reaching the surface becomes restricted, they deviate from the external heat delivered  
97 to the surface may become much higher than the energy required for the evaporation process.  
98 This induces overheating and casehardening with over consumption of energy and loss of  
99 quality.

100 Thus, the Interval Highly Active Drying (IHAD) processes have been defined as means of  
101 short intervals capable of closely controlling drying efficiency, separating the heat input with  
102 the water to be evaporated from the surface (French Patent of Mounir et al. (2017)). During  
103 interval drying, the heat source is ON (active period) only for few seconds to permit the  
104 evaporation of surface water, and is OFF (tempering time) to allow the internal water to  
105 diffuse and reach the exchange surface (Hajji et al., 2020). It is worth noticing that the  
106 conventional intermittent drying described in the literature uses prolonged active period and  
107 tempering times, of several minutes to several hours (Chin & Law, 2010; Silva et al., 2016;  
108 Tetang Fokone, Marcel, & Alexis, 2020; Yang, Zhu, Zhu, Wang, & Li, 2013). The minimum

109 intermittent tOFF observed in the literature was 6 min with 40 s as active time for Chinese  
110 cabbage seeds (Yang et al., 2013).

111 Improving the dried product quality, saving energy, reducing emissions, and increasing  
112 efficiency are the most desirable objectives in industrial processes. Hence, such an innovative  
113 drying process was proposed, set up, and tested on convective drying (Hajji et al., 2020). By  
114 using IR radiation as an intensive heat source for evaporating the superficial water combined  
115 with the transport of the vapor, this Interval IR airflow Drying (IIRAD) process is based on  
116 IHAD.

117 Therefore, the main objectives of this work were to control the drying parameters of energy  
118 input and to highlight the effects of the active and tempering times in the specific case of  
119 butternut drying. The efficiency of the IIRAD mode and conditions on preserving (or not) of  
120 the product quality were also analyzed.

## 121 **2. Materials and Methods**

### 122 **2.1. Biological Materials**

123 Butternut squash (*Cucurbita moschata*) was purchased from a local supermarket in La  
124 Rochelle, France. The squash samples were hand-peeled and cored, and then cut into  
125 parallelepiped of  $(4.6 \pm 0.1) \times (10 \pm 0.4) \times (50 \pm 0.5)$  mm<sup>3</sup>. To determine the initial sample moisture  
126 content, samples of 5 g were placed in the oven for 24 h at 105 °C until constant weight.

### 127 **2.2. Drying experiments**

128 The new drying mode IIRAD was implemented using infrared energy coupled with ambient  
129 temperature ( $18 \pm 1$  °C) airflow ( $1.41$  m s<sup>-1</sup>) drying. Three modes of IR/air-convection were  
130 tested in this work: (i) conventional IR drying, (ii) I-IIRAD with constant active and  
131 tempering times, and (iii) II-IIRAD with variable active time  $t_{ON}$  and constant tempering time

132  $t_{\text{OFF}}$ . These drying modes were compared in terms of drying kinetics, bulb-temperature,  
133 energy consumption, and quality of the dried products.

### 134 **2.2.1. Drying apparatus**

135 The drying experiments were conducted with an infrared dryer/ambient temperature airflow  
136 specific device (Fig.1). The IR irradiation was emitted by three lamps suspended in the upper  
137 part of the drying chamber with a maximum power of  $4 \text{ W cm}^{-2}$ , which was adjusted using an  
138 equipment variator. A fan was placed above the lamps and the airflow velocity at the product  
139 was maintained at  $1.48 \text{ m s}^{-1}$ .

### 140 **2.2.2. IR drying Experiments**

141 Preliminary tests led to the selection of  $0.7 \text{ W.cm}^{-2}$  as IR power. The squash samples were  
142 placed in the drying chamber on a perforated tray, 7.5 cm from the IR sources. The evolution  
143 of squash sample mass during the drying process was measured using a balance (RADWAG,  
144 PS2500.3Y, Poland) with 0.01 g accuracy to obtain the evolution of the moisture content  
145 versus drying time, with the conventional continuous IR drying mode as a reference.

146 At this level of IR power, the IIRAD intervals were defined by a very short active time ( $t_{\text{ON}}$ )  
147 capable exclusively of vaporizing exactly the surface water, followed by a time ( $t_{\text{OFF}}$ )  
148 allowing the water transfer and homogenization within the matrix (Fig. 2). Thus, the  
149 experiment consisted in exposing the squash samples to IR heating for a few seconds of  $t_{\text{ON}}$ ,  
150 then standing them for a tempering time ( $t_{\text{OFF}}$ ) to allow the water to diffuse from the deepest  
151 zone to the exchange surface of the sample matrix. Energy is then adequately used during  $t_{\text{ON}}$   
152 to evaporate water at the surface, while  $t_{\text{OFF}}$  interval, defined to allow re-wetting of the surface  
153 and homogenization of the water distribution in the product, does not involve any energy  
154 consumption. The actual duration of the drying operation during which the IR is activated is  
155 particularly reduced (Hajji et al., 2020).

156 Two sets of IIRAD operating conditions were tested. I-IIRAD was performed with a constant  
157 active time,  $t_{ON}=5$  s. The tempering time  $t_{OFF}$  was selected as  $t_{OFF}=2$  min. This value derives  
158 from previously obtained results of fundamental and experimental studies of Interval Starting  
159 Accessibility Drying (ISAD). Indeed,  $t_{OFF}$  between 2 and 3 minutes has been estimated to be  
160 sufficient to allow water to diffuse towards the surface when using the same sample sizes.

161 To take into account the decrease in water content during drying, II-IIRAD was set up with a  
162 variable  $t_{ON}$  during the drying process according to the residual water content, while  $t_{OFF}$  was  
163 maintained constant (2 min). Thus, II-IIRAD operation was divided into three parts according  
164 to moisture content intervals. These parts durations are set up in the results section.

### 165 **2.2.3. Energy Consumption**

166 In this study,  $t_{ON}$  was initially estimated at 5 s. Thus, the initial  $t_{ON}$  infrared energy  $Q_{t_{ON}}$  is  
167 determined using the following formula (Eq.1):

$$Q_{t_{ON}} = P \cdot t_{ON} \quad \text{Eq. 1}$$

168 Where P is the infrared power ( $\text{kW m}^{-2}$ ) and  $t_{ON}$  is expressed in (s).

169 In this case, assuming that the whole IR energy was used for evaporating the superficial water  
170  $m_{v,t_{ON}}$  which is calculated as (Eq. 2):

$$m_{v,t_{ON}} = Q_{t_{ON}}/L_v \quad \text{Eq. 2}$$

171 Where  $L_v$  is the water latent heat of vaporization ( $2444 \text{ kJ kg}_{\text{vapor}}^{-1}$ ) as calculated from  
172 (Rogers & Yau, 1989) equation:

$$L_v = 2500.8 - 2.36T + 0.0016T^2 - 0.00006T^3 \quad \text{Eq. 3}$$

173 where  $L_v$  is expressed in  $kJ/kg$  vapor  $H_2O$  and  $T$  in  $^{\circ}C$ . The specific energy consumption  $E_s$   
 174 per kg of vapor for the total drying process is calculated (Eq. 3) according to Salarikia, Miraei  
 175 Ashtiani, and Golzarian (2017):

$$E_s = E_t/m_v = \frac{PA t}{m_v} \quad \text{Eq. 4}$$

176 Where  $A$  is the sample area ( $m^2$ ),  $m_v$  ( $kg$   $H_2O$ ) the amount of generated vapor during the  
 177 effective drying time  $t$ , and  $E_t$  is the total IR energy consumption.

### 178 **2.3. Temperature assessments**

179 The airflow and bulb temperatures during the whole drying process were measured using  
 180 thermocouples (CENTER-304 type k). The sample probe was placed into the squash sample  
 181 at about 2-2.5 mm from the surface.

### 182 **2.4. Product temperature profile**

183 Systematically, a drying operation involves supplying a quantity of heat, which, in the case of  
 184 airflow convection, is  $Q_a$  (Eq. 4):

$$dQ_a = dQ_{convection} = hS(T_{air} - T_{b,s})dt \quad \text{Eq. 5}$$

185 Where  $h$  is heat transfer coefficient ( $W$   $m^{-2}$   $K^{-1}$ );  $S$  total area ( $m^2$ );  $T_{air}$  convective air  
 186 temperature ( $K$ );  $T_{b,s}$  bulb/surface temperature ( $K$ ), and  $t$  is the time ( $s$ ).

187 In the case of IR heating source, the amount of heat absorbed by the surface of the material  
 188 (Eq. 5) is related to the material emissivity and the exchange surface, and it is assumed to be  
 189 correlated to the IR source temperature.

$$dQ_a = dQ_{IR} = \varepsilon\sigma S(T_{IR}^4 - T_{b,s}^4)dt \quad \text{Eq. 6}$$

190 Where  $\varepsilon$  is the surface emissivity, the Stefan-Boltzmann constant  $\sigma=5.67.10^{-8}$  W m<sup>-2</sup> K<sup>-4</sup>, and  
 191  $T_{IR}$  and  $T_{b,s}$  are the source infrared and the product surface temperatures, respectively.  
 192 In conventional drying operations, the heat received by the material is primarily used to  
 193 evaporate water from the surface, to reach the equilibrium vapor concentration in the  
 194 surrounding medium (Eq. 6).

$$dQ_v = dm_v L_v \quad \text{Eq. 7}$$

195 Where  $dQ_v$  is the amount of evaporation heat and  $dm_v$  the vapor generated during time dt  
 196 while  $L_v$  is the evaporation latent heat. The residual heat is then transferred by conduction to  
 197 be used in sensible form to modify the material temperature (Eq. 7):

$$dQ_b = m_d(c_{p,d} + Wc_{p,w})dT_b \quad \text{Eq. 8}$$

198 Where  $dQ_b$  is the amount of sensible heat absorbed by the bulb,  $m_d$  and  $W$  are the dry and  
 199 water contents of the bulb matter dry basis, respectively;  $c_{p,d}$  and  $c_{p,w}$  are the specific heat of  
 200 dry matter and water, respectively, and  $dT_b$  the bulb temperature evolution during time dt. The  
 201 residual heat  $dQ_b$  is related to  $dQ_{IR}$  and  $dQ_v$  by conduction as follows (Eq. 8 and Eq. 9):

$$dQ_b = d(Q_{IR} - Q_v) \quad \text{Eq. 9}$$

$$dT_b = \frac{(\dot{Q}_{IR} - \dot{Q}_v)}{m_d(c_{p,d} + Wc_{p,w})} dt \quad \text{Eq. 10}$$

## 202 **2.5. Quality parameters determination**

### 203 **2.5.1. Color**

204 Color analyses for fresh and infrared-dried squash samples were performed using a  
 205 Chromameter (Konica Minolta CR-410, Tokyo, Japan) on four randomly selected pieces at  
 206 different locations. Three parameters (lightness L, redness a, and yellowness b) were

207 investigated as positive value (+). The total color difference ( $\Delta E_c$ ) between the fresh and dried  
208 butternut samples was calculated (Eq. 10) as:

$$\Delta E_c = \sqrt{(L_0 - L^*)^2 + (a_0 - a^*)^2 + (b_0 - b^*)^2} \quad \text{Eq. 11}$$

209 Where the subscripts “o” and “\*” refer to the color parameters of fresh and dried squash  
210 samples, respectively.

### 211 **2.5.2. Total Polyphenol and total flavonoids content**

212 The colorimetric methods were achieved to determine the total polyphenol (TPC) and total  
213 flavonoid (TFC) contents as described by Ben Haj Said, Najjaa, Neffati, and Bellagha (2013).  
214 TPC of squash slices was determined using Gallic acid and the (TFC) was measured using  
215 quercetin as a standard.

### 216 **2.5.3. Rehydration process**

217 Approximately 0.2 g of dried product was placed in a glass beaker containing distilled water  
218 at 25 °C. The change in mass during rehydration was measured using an electronic balance.  
219 At predefined time intervals, the dried samples were taken and buffered with absorbent paper  
220 to remove excess water from the surface. For the first five minutes, weight measurements  
221 were taken every minute, followed by every 5 minutes during 15-minute period, and then one  
222 measurement at 10 minutes. The rehydration ratio (RR) was calculated (Eq. 11) according to  
223 Lewicki (1998):

$$RR = \frac{\text{Mass of rehydrated sample} - \text{Mass of dried sample}}{\text{Mass of dried sample}} \quad \text{Eq. 12}$$

## 224 **2.6. Statistics**

225 The statistical analysis of data was determined using statgraphics centurion 18 version  
226 18.1.12. The significance of difference among means was achieved through ANOVA tests.

227 The analyzes were carried out in triplicate and the values are presented as the mean  $\pm$  standard  
228 deviation (SD).

## 229 **3. Results and Discussion**

### 230 **3.1. IIRAD operating conditions**

231 IIRAD operating parameters i.e., the active and tempering times depend on the sample initial  
232 moisture content, water diffusivity, thickness, and IR power. Hence, a main part of this work  
233 consisted in setting up a procedure to estimate  $t_{ON}$  and  $t_{OFF}$  to use with IIRAD. The three  
234 various drying operations of this work; the continuous IR drying mode, I-IIRAD (Constant  
235  $t_{ON}=5$  s,  $t_{OFF}=2$  min), and II-IIRAD with a variable active time and a constant tempering time.  
236 Based on the drying behavior of the squash samples as described by the drying curve (Fig. 3)  
237 obtained under continuous IR drying, active time durations for II-IIRAD were selected as  
238 follow: Constant  $t_{OFF}=2$  min while  $t_{ON}$  varying from (i) 5 s during the first 240 min with water  
239 content evolved from  $W=9$  till  $W=4$  g  $H_2O/g$  db), (ii)  $t_{ON}=4$  s for 273 min of total time (till  
240  $W=2.6$  g  $H_2O/g$  db), and finally (iii)  $t_{ON}=2$  s till the end of the process. These operations were  
241 performed to evaluate their respective effects on active time kinetics, energy consumption,  
242 and product quality. The different drying kinetics obtained are shown in Fig. 3.

243 During interval drying, each active interval is carried out to produce more easily the  
244 evaporation for a very short period time. The continuation of the process during a subsequent  
245 step of too weak concentration of water on the exchange surface, induces a reduction in  
246 kinetics, a casehardening and, thus, a greater consumption of energy and a loss of quality. On  
247 the other hand, if a simple stop in the drying process takes place, only the diffusion occurs to  
248 make a more uniform water distribution within the material. It results in a marked  
249 improvement in the match between material and process. These successive intervals of  
250 evaporation and diffusion define various "interval drying" processes.

251 Indeed, whereas conventional drying usually involves both mechanisms i.e., surface  
252 evaporation and water diffusion, simultaneously, IIRAD's fundamental approach is to  
253 dissociate surface evaporation and internal water diffusion in successive intervals. Thus, the  
254 first interval is defined as the evaporation time of surface moisture, while the second interval  
255 depends on the diffusivity of the natural matrix and cell structure as well as the sample size.  
256 In conventional drying processes, heating is maintained while the internal diffusion of water  
257 doesn't allow the water to completely reach the exchange surface. Hence, a large part of the  
258 energy is used to heat the material, degrade the nutritional and active molecules, and extend  
259 the effective drying time.

### 260 **3.2. Drying kinetics**

261 Squash samples were dried from the initial moisture content of  $9.04 \pm 0.12$  towards an  
262 unchanged mass which corresponds to a final water content of  $0.27 \pm 0.02$  g H<sub>2</sub>O/g db after  
263 80 min, 35 min, and 28 min of effective drying for continuous IR, type I-IIRAD, and type II-  
264 IIRAD, respectively (Fig. 3). The moisture content rapidly decreased during IIRAD type I and  
265 II compared to continuous IR drying. These observations were also made by (Hajji, Bellagha,  
266 & Allaf, 2020) during interval convective drying (Interval Starting Accessibility Drying,  
267 ISAD) of quince. IIRAD type I and II curves are confounded for the most part of the kinetics.  
268 However, at the end of IIRAD Type II drying curve, a higher evaporation rate is noted.  
269 Therefore, reducing  $t_{ON}$  from 5 to 2 s has a positive effect on drying.

270 By completely separating the two mechanisms of IR heating and water diffusion, and by  
271 adopting a sufficient tempering period  $t_{OFF}$  for a complete surface rewetting, IIRAD results in  
272 decreasing the “bulb temperature” as low as the evaporating rate is high (Fig. 4 and Fig 5).  
273 Moreover, as casehardening is normally correlated with high temperature/large time drying  
274 processes, this new treatment involving low temperature/short time should greatly reduce the  
275 risks of casehardening formation. Hence, the adequate evaluation of  $t_{OFF}$  to let the internal

276 water diffuse toward the surface, facilitates the water removal by evaporation during  $t_{ON}$ . This  
277 resulted in a higher effective drying rate for IIRAD processes (Fig. 3).

278 The two curves, obtained by both types I and II IIRAD, followed similar trends as much as in  
279 the first 20 min of effective drying time. The change of active time from 5 s to 4 s and finally  
280 to 2 s, did not significantly modify the water elimination rates of I-IIRAD and II-IIRAD which  
281 were 0.333 and 0.357 g H<sub>2</sub>O g<sup>-1</sup> db min<sup>-1</sup>, respectively.

282 However, the slowdown at the final stage of I-IIRAD (fig. 3) means that  $t_{ON}$  of 5 s at this  
283 stage of the drying process, was too long and water diffusion during  $t_{OFF}$  didn't bring enough  
284 water to the surface. In the contrary, by decreasing  $t_{ON}$  to 2 s during this last stage of II-  
285 IIRAD, the 2-min  $t_{OFF}$  allowed sufficient rehydration of the surface. This result justifies the  
286 lower value of active time chosen during II-IIRAD.

287 Sun et al. (2020) compared intermittent IR drying using 6 h and 4 h for  $t_{ON}$ , and  $t_{OFF}$   
288 maintained at 1 h with continuous drying and obtained similar kinetics, contrary to what is  
289 observed in this IIRAD study (Fig. 3). They still observe more uniform moisture distribution  
290 after the tempering time and even at the end of drying. When using a shorter  $t_{ON}$  of 4 h and a  
291  $t_{OFF}$  of 1 h, they observed lower water content gradient and better humidity homogenization,  
292 thus obtaining better drying than continuous drying and intermittent with a  $t_{ON}$  of 6 h.

293 Finally, it is worth noting that during the last minutes of IIRAD Types I and II, a slight  
294 slowing down of the drying rate was observed. This period may also be correlated to the  
295 paradoxical step in which water is evaporated within the volume and the vapor is transferred  
296 from high-temperature zone (near the exchange surface) towards the core as explicitly  
297 described.

### 298 3.3. Product temperature profile

299 Even though the water content appears in Eq. 9, it is clear that product “wet” bulb temperature  
300 doesn’t greatly depend on the water content; it is predominantly function of drying rate  $\dot{Q}_v$ .  
301 Indeed, it is clear in this work that the higher the drying evaporating rate, the lower the  
302 “Evaporating-Bulb Temperature  $T_b$ ”. Thus, during the active period  $t_{ON}$ , once  $Q_{IR}$  is  
303 approximately completely used for evaporating the water at the surface  $Qv = m_v L_v$ , the  
304 difference between the bulb and the initial ambient temperatures  $\Delta T_b$  is close to zero.

305 Fig 4 exemplifies the temperature profiles during the continuous IR drying, and both types I-  
306 IIRAD and II-IIRAD inside the squash pieces. The bulb temperature  $T_b$  of the continuous IR  
307 drying product, increased sharply from ambient temperature towards about 66 °C, in  
308 agreement with Hashimoto and Kameoka (1999) studies. In both cases of IIRAD,  $T_b$  kept  
309 approximately constant and did not exceed 21 °C. In this way, IIRAD types avoided  
310 overheating throughout drying. In the various other types of conventional intermittent drying  
311 operations, bulb-product temperature remains high, not because of higher heating time , but  
312 specifically because of low evaporation rate.

313 Hence, during the convective drying of pears, with several hours as  $t_{ON}$  and 1 hour minimum  
314 as  $t_{OFF}$ , Silva et al. (2016) deduced that the first tempering period allowed the sample to cool  
315 but then subsequent  $t_{OFF}$  periods had no longer significant effect on the reduction of the  
316 internal and surface temperature of the samples. Exposing alternatively, sweet potato samples,  
317 to IR heating for 2 min and to convective drying during 4 min, resulted in bulb temperature  
318 rise reaching 90-95 °C.

319 Other correlations of the evolution rate of the evaporating bulb temperature  $T_b$  versus the  
320 evaporation rate  $\dot{m}_v$  were established (Figure 5).

321 Figure 5 clearly shows that evaporating bulb temperature evolution as a function of the  
322 evaporation rate follows a decreasing profile during conventional drying and is almost  
323 constant during the two types of IIRAD. The curve related to continuous drying showing a  
324 decrease in drying rate, implied higher bulb temperature. In the contrary, despite a high-water  
325 removal rate, product bulb temperature variation is very low during IIRAD kinetics, which is  
326 in line with the fundamental results established above in Eq. 9. The bulb temperature depends  
327 predominantly on drying rate. Thus, the almost nil variation in temperature is due to the use of  
328 the energy received by the sample during  $t_{ON}$  for evaporating water and not for heating.

329 Low  $t_{ON}$  values and a compromise between  $t_{ON}$  and  $t_{OFF}$  should be defined to allow the water  
330 to adequately reach the surface during  $t_{OFF}$  and avoid any weak evaporating rate during the  
331 active IR heating. Temperature is well known as a key factor in accelerating drying kinetics.  
332 However, overheating should be avoided to preserve, among others, nutrients. In conventional  
333 intermittent infrared with a cycle time of 30 min, Chua and Chou (2005) explain that the  
334 surface of the samples is rewet during  $t_{OFF}$ ; the superficial vapor generation protects the  
335 samples from overheating. The higher the sample surface evaporation, the lower the bulb  
336 temperature. Although the intermittence reduces the overheating, long  $t_{ON}$  periods normally  
337 induce temperature rises. The results of Chin and Law (2010) study illustrated that extended  
338  $t_{ON}$  and  $t_{OFF}$  periods, from 120 to 240 min, don't allow high evaporation rate and low bulb  
339 temperature, nor preserving nutritional or sensitive molecules. IIRAD has the specificity of  
340 avoiding all these negative drying impacts.

### 341 **3.4. Energy consumption**

342 Although IR drying includes some part of mechanical airflow energy, the specific energy  
343 consumption of the three modes of IR drying tested in this work, i.e. continue IR process, and  
344 types I and II-IIRAD are chiefly limited and mostly related to IR energy amount with  
345 insignificant amount of the other energy types (Table 1). In these three IR drying types, the IR

346 power was kept constant at  $0.7 \text{ W/cm}^2$  and the effective drying times were 80, 35, and 28 min,  
347 respectively. This involves 2.19, 0.97, and 0.77 kWh/kg  $\text{H}_2\text{O}$  (Fig. 6), respectively. As it can  
348 be seen, IIRAD drying process considerably decreases the energy consumption compared to  
349 the continuous mode (Fig. 6). This observation is completely linked with the effective drying  
350 time. Thus, the shorter the effective drying time, the lower the drying energy consumption.  
351 This is clear since IIRAD undergoes much higher active evaporation rate, without any  
352 significant lateral heating energy or quality degradation. Hence, by adjusting  $t_{\text{ON}}$  adequately to  
353 the superficial water evaporation needs, and  $t_{\text{OFF}}$  to the product specific transfer parameters  
354 (diffusivity, water content, thickness...) to allow the internal water to diffuse within the whole  
355 matrix, IIRAD led to shorter effective drying durations and lower power consumption.

356 Salarikia et al. (2017) observed that the intensification of conventional IR drying would  
357 require increasing infrared intensity, air temperature, or the combination of these two aspects.  
358 Such an intensification makes it possible reducing both drying time and energy losses.  
359 Furthermore, since IR heating provided more directly absorbed energy by the sample surface,  
360 the energy losses for heating the ambient air were insignificant. Hebbar et al. (2004) found  
361 that the combined convective hot air with infrared allowed reducing by 62% the drying time  
362 of potatoes and a reduction of energy consumption from 17.17 to 6.43 MJ/kg (or 4.769 to  
363 1.786 kWh/kg of evaporated water) (Fig 6).

### 364 **3.5. Quality parameters**

#### 365 **3.5.1. Rehydration rate**

366 Rehydration Ratios (RRs) of the samples dried by different methods were calculated using  
367 Eq. (11). In Fig.7, the continuous IR drying showed higher RR than IIRAD ( $P < 0.05$ ).

368 Rehydration behaviors are considered as a relevant indicator of quality, normally related to  
369 the irreversible damage caused by the drying on the plant tissues. Structural and chemical

370 changes undergone during dehydration may be explained by the rehydration ratio (RR).  
371 Rehydration capacity is directly related to the extent of the cellular membrane disruption as  
372 well as to the biochemical changes such as polysaccharides crystallization and solute  
373 migration. As these phenomena are temperature dependent, higher RR are observed  
374 throughout continuous IR drying which undergoes the highest temperatures and could induce  
375 major breakage of cell walls allowing a faster water flow and a higher absorption capacity  
376 during the rehydration process.

377 It is worth differentiating the RR from the water holding capacity (WHC). Indeed, Vega-  
378 Galvez et al. (2015) observed that drying Cape gooseberry at 50 °C allowed obtaining lower  
379 RR and higher WHC compared to samples dried at higher temperatures (70-90 °C). The lower  
380 the drying temperature, the better preserved the structure.

### 381 **3.5.2. Effect of drying modes on color measurements of squash pieces**

382 Several quality parameters of the dried product were investigated (Table 2) at similar final  
383 water contents ranging from 0.27, 0.21, and 0.26 g H<sub>2</sub>O/g db for continue IR, Type II-IIRAD,  
384 and Type I-IIRAD, respectively. Hence, the three types of IR dried samples were compared in  
385 terms of color parameters (L, a, b, and ΔE), and total polyphenol and total flavonoid contents  
386 (Table 2).

387 The fresh squash had a light orange color with L\*, a\*, and b\* of 79.98, 10.79 and 26.53,  
388 respectively. IR drying exerted a significant effect on the squash color. A pronounced  
389 degradation was observed after the continuous process, which significantly affected ΔE at  
390 20.77 against 9.42 and 9.66 for the interval drying modes I-IIRAD and II-IIRAD,  
391 respectively. The color preservation was directly related to the squash temperature (Fig. 5).  
392 Since the surface sample undergoes even higher temperature, continuous IR brings more  
393 pigment denaturation. Alaei and Chayjan (2015) had similar observations when drying of

nectarines at ranging from 60 to 90 °C, brought the least color difference for the lowest temperature of 60 °C.

### 3.5.3. Effect of drying modes on total phenolic and total flavonoid contents of squash pieces

The lower loss in total polyphenol content (TPC) was observed in the continuous IR dried samples with values of  $42.70 \pm 2.75$  against  $48.42 \pm 0.91$  and  $47.18 \pm 2.98$  mg GAE/100 g db for II-IIRAD and I-IIRAD, respectively (Table 2). These results may be related to the temperature experienced by the product. Indeed, Potosí-Calvache, Vanegas-Mahecha, and Martínez Correa (2017) found that the TPC content increased from  $37.1 \pm 2.6$  to  $41.0 \pm 1.2$  mg GAE/100 g of squash (*Cucurbita moschata*) sample when the temperature increased from 65 to 69 °C. Bochnak and Świeca (2019) obtained similar results and found higher TPCs ( $7.85 \pm 1.01$  mg GAE/g db) in pumpkin flour after drying at 70 °C than that dried at 50 °C ( $4.35 \pm 0.44$  mg GAE/ g powders). Furthermore, Que, Mao, Fang, and Wu (2008) observed phenolic substance formation at high drying temperatures of 70 °C in pumpkin. This corroborates our results since the highest TPC were gotten for continuous dried samples with 66 °C while IIRAD didn't exceed 25 °C.

The total flavonoid content undergone important loss under all IR drying processes (Table 2). Contrary to total polyphenols, the lowest total flavonoid level was obtained after continuous IR drying with a 68.08% loss. The higher the bulb temperature beyond 60°C during the continuous IR drying, the higher the flavonoid content loss. The total flavonoid content depends on the drying temperature, solvent, and extraction mode according to Tiho, Yao, Brou, and Adima (2017). Sukrasno, Fidrianny, Anggadiredja, Handayani, and Anam (2011) studying *Cosmos caudatus* (Kunth) leaves found that air heating at temperatures varying from 30 to 100 °C decreased the total flavonoid content. An exception observed at 40 °C was

418 explained by enzyme degradation, which reaches its optimum activity at a temperature of 50  
419 °C.

#### 420 **4. Conclusion**

421 A new drying process entitled IIRAD was applied to drying of butternut pieces to assess its  
422 efficiency in terms of the drying kinetics, energy consumption and quality. Results showed  
423 that the two types of IIRAD performed at fixed and variable  $t_{ON}$  allowed reduction both  
424 drying time and energy consumption. Energy savings was between 55-65% of that needed by  
425 continuous IR drying. IIRAD allows drying time to be lowered thanks to the tempering time  
426 which allows adequate rewetting of the sample surface. Here water reaching the upper layers  
427 is more easily evaporated during  $t_{ON}$ , which accelerates the effective drying rate. Thus, the  
428 surface temperature is maintained low throughout the IIRAD process.

429 IIRAD treatment resulted in better preservation of the TFC and visual appearance of the dried  
430 product. IIRAD conditions can intensify the elimination of water, reduce drying time, and  
431 improve several quality attributes of the final product. It is worth noting the importance of  
432 modulating  $t_{ON}$  as a function of the residual product water content during drying and  $t_{OFF}$   
433 depending on the water diffusivity and sample size to optimize the process.

434

## 435 **Uncategorized References**

- 436 Alaei, B., & Chayjan, R. (2015). Modelling of nectarine drying under near infrared – Vacuum  
437 conditions. *Acta Scientiarum Polonorum Technologia Alimentaria*, 14, 15-27.  
438 doi:10.17306/J.AFS.2015.1.2
- 439 Allaf, K., Mounir, S., Negm, M., Allaf, T., Ferrasse, H., & Mujumdar, A. (2014). Intermittent  
440 Drying. In (pp. 33).
- 441 Allaf, T., Allaf, K. Instant Controlled Pressure Drop (D.I.C.) in Food Processing: From  
442 Fundamental to Industrial Applications; Food engineering series; Springer: New York,  
443 2014
- 444 Armesto, J., Rocchetti, G., Senizza, B., Pateiro, M., Barba, F. J., Dominguez, R.,... Lorenzo, J.  
445 M. (2020). Nutritional characterization of Butternut squash (*Cucurbita moschata* D.):  
446 Effect of variety (Ariel vs. Pluto) and farming type (conventional vs. organic). *Food*  
447 *Res Int*, 132, 109052. doi:10.1016/j.foodres.2020.109052
- 448 Beigi, M. (2017). Thin layer drying of wormwood (*Artemisia absinthium* L.) leaves:  
449 dehydration characteristics, rehydration capacity and energy consumption. *Heat and*  
450 *Mass Transfer*, 53 (8), 2711-2718. doi:10.1007/s00231-017-2018-3
- 451 Ben Haj Said, L., Najjaa, H., Neffati, M., & Bellagha, S. (2013). Color, Phenolic and  
452 Antioxidant Characteristic Changes of *Allium Roseum* Leaves during Drying. *Journal*  
453 *of Food Quality*, 36 (6), 403-410. doi:https://doi.org/10.1111/jfq.12055
- 454 Bochnak, J., & Świeca, M. (2019). Potentially bioaccessible phenolics, antioxidant capacities  
455 and the colour of carrot, pumpkin and apple powders – effect of drying temperature  
456 and sample structure. *International Journal of Food Science & Technology*, 55 (1),  
457 136-145. doi:10.1111/ijfs.14270

- 458 Chin, S. K., & Law, C. L. (2010). Product Quality and Drying Characteristics of Intermittent  
459 Heat Pump Drying of *Ganoderma tsugae* Murrill. *Drying Technology*, 28 (12), 1457-  
460 1465. doi:10.1080/07373937.2010.482707
- 461 Chua, K. J., & Chou, S. K. (2005). A comparative study between intermittent microwave and  
462 infrared drying of bioproducts. *International Journal of Food Science and Technology*,  
463 40 (1), 23-39. doi:10.1111/j.1365-2621.2004.00903.x
- 464 Dongbang, W., & Matthujak, A. (2013). Anchovy Drying Using Infrared Radiation. *American*  
465 *Journal of Applied Sciences*, 10, 353-360.
- 466 Doymaz, I., Kipcak, A. S., & Piskin, S. (2016). Characteristics of thin-layer infrared drying of  
467 green bean. *Czech Journal of Food Sciences*, 33 (No. 1), 83-90.  
468 doi:10.17221/423/2014-cjfs
- 469 Fernando, W., Low, H., & Ahmad, A. L. (2011). The Effect of Infrared on Diffusion  
470 Coefficients and Activation Energies in Convective Drying: A Case Study for Banana,  
471 Cassava and Pumpkin. *Journal of Applied Sciences*, 11, 3635-3639.  
472 doi:10.3923/jas.2011.3635.3639
- 473 Ghaboos, S. H., Ardabili, S. M., Kashaninejad, M., Asadi, G., & Aalami, M. (2016).  
474 Combined infrared-vacuum drying of pumpkin slices. *J Food Sci Technol*, 53 (5),  
475 2380-2388. doi:10.1007/s13197-016-2212-1
- 476 Hajji, W., Bellagha, S., & Allaf, K. (2020). Energy-saving new drying technology: Interval  
477 starting accessibility drying (ISAD) used to intensify dehydrofreezing efficiency.  
478 *Drying Technology*, 1-15. doi:10.1080/07373937.2020.1788072
- 479 Hashimoto, A., & Kameoka, T. (1999). Effect of Infrared Irradiation on Drying  
480 Characteristics of Wet Porous Materials. *Drying Technology*, 17 (7-8), 1613-1626.  
481 doi:10.1080/07373939908917640

482 Hebbar, H. U., Vishwanathan, K. H., & Ramesh, M. N. (2004). Development of combined  
483 infrared and hot air dryer for vegetables. *Journal of Food Engineering*, 65 (4), 557-  
484 563. doi:10.1016/j.jfoodeng.2004.02.020

485 Ismail, O. (2016). Effects of Drying Methods on Drying Characteristic, Energy Consumption  
486 and Color of Nectarine. *Journal of Thermal Engineering*, 2. doi:10.18186/jte.00886

487 Kayran, S., & Doymaz, İ. (2017). Infrared Drying and Effective Moisture Diffusivity of  
488 Apricot Halves: Influence of Pretreatment and Infrared Power. *Journal of Food*  
489 *Processing and Preservation*, 41 (2), e12827. doi:10.1111/jfpp.12827

490 Krokida, M. K., & Philippopoulos, C. (2005). Rehydration of Dehydrated Foods. *Drying*  
491 *Technology*, 23 (4), 799-830. doi:10.1081/DRT-200054201

492 Kumar, C., Millar, G. J., & Karim, M. A. (2014). Effective Diffusivity and Evaporative  
493 Cooling in Convective Drying of Food Material. *Drying Technology*, 33 (2), 227-237.  
494 doi:10.1080/07373937.2014.947512

495 Lewicki, P. P. (1998). Some remarks on rehydration of dried foods. *Journal of Food*  
496 *Engineering*, 36 (1), 81-87. doi:https://doi.org/10.1016/S0260-8774 (98)00022-3

497 Moses, J. A., Norton, T., Alagusundaram, K., & Tiwari, B. K. (2014). Novel Drying  
498 Techniques for the Food Industry. *Food Engineering Reviews*, 6 (3), 43-55.  
499 doi:10.1007/s12393-014-9078-7

500 Mounir, S., Ben Haj Said, L., Allaf, T., Hajji, W., Negm, M., & Bellagha, S. (2017). France  
501 Patent No. Institutue National de la propriété industrielle: S. c. i. e. m. d. s. (C.I.M.S).

502 Mounir, S., Besombes, C., Al-Bitar, N., & Allaf, K. (2011). Study of Instant Controlled  
503 Pressure Drop DIC Treatment in Manufacturing Snack and Expanded Granule Powder  
504 of Apple and Onion. *Drying Technology*, 29, 331-341.  
505 doi:10.1080/07373937.2010.491585

- 506 Mounir, S., Téllez-Pérez, C., Alonzo-Macías, M., & Allaf, K. (2014). Swell-Drying. In (pp. 3-  
507 43).
- 508 Official methods of analysis, (1999)
- 509 Onwude, D. I., Hashim, N., Abdan, K., Janius, R., & Chen, G. (2019). Experimental studies  
510 and mathematical simulation of intermittent infrared and convective drying of sweet  
511 potato (*Ipomoea batatas* L.). *Food and Bioproducts Processing*, 114, 163-174.  
512 doi:10.1016/j.fbp.2018.12.006
- 513 Pawar, S. B., & Pratape, V. M. (2017). Fundamentals of Infrared Heating and Its Application  
514 in Drying of Food Materials: A Review. *Journal of Food Process Engineering*, 40 (1),  
515 e12308. doi:10.1111/jfpe.12308
- 516 Potosí-Calvache, D. C., Vanegas-Mahecha, P., & Martínez Correa, H. A. (2017). Convective  
517 drying of squash (*Cucurbita moschata*): Influence of temperature and air velocity on  
518 effective moisture diffusivity, carotenoid content and total phenols. *Dyna*, 84 (202),  
519 112-119. doi:10.15446/dyna.v84n202.63904
- 520 Que, F., Mao, L., Fang, X., & Wu, T. (2008). Comparison of hot air-drying and freeze-drying  
521 on the physicochemical properties and antioxidant activities of pumpkin (*Cucurbita*  
522 *moschata* Duch.) flours. *International Journal of Food Science & Technology*, 43 (7),  
523 1195-1201. doi:10.1111/j.1365-2621.2007.01590.x
- 524 Ratti, C., & Mujumdar, A. (2006). *Infrared Drying*. doi:10.1201/9781420017618.ch18
- 525 Rogers, R. R., & Yau, M. K. (1989). *A Short course in cloud physics*. Burlington, Mass.:  
526 Butterworth Heinemann.
- 527 Salarikia, A., Miraei Ashtiani, S.-H., & Golzarian, M. R. (2017). Comparison of Drying  
528 Characteristics and Quality of Peppermint Leaves Using Different Drying Methods.  
529 *Journal of Food Processing and Preservation*, 41 (3), e12930. doi:10.1111/jfpp.12930

- 530 Samadi, S. H., & Loghmanieh, I. (2013). Evaluation of Energy Aspects of Apple Drying in  
531 the Hot-Air and Infrared Dryers.
- 532 Shi, J., Pan, Z., McHugh, T. H., Wood, D., Hirschberg, E., & Olson, D. (2008). Drying and  
533 quality characteristics of fresh and sugar-infused blueberries dried with infrared  
534 radiation heating. *LWT - Food Science and Technology*, 41 (10), 1962-1972.  
535 doi:<https://doi.org/10.1016/j.lwt.2008.01.003>
- 536 Silva, V., Costa, J. J., Figueiredo, A. R., Nunes, J., Nunes, C., Ribeiro, T. I. B., & Pereira, B.  
537 (2016). Study of three-stage intermittent drying of pears considering shrinkage and  
538 variable diffusion coefficient. *Journal of Food Engineering*, 180, 77-86.  
539 doi:[10.1016/j.jfoodeng.2016.02.013](https://doi.org/10.1016/j.jfoodeng.2016.02.013)
- 540 Sui, Y., Yang, J., Ye, Q., Li, H., & Wang, H. (2014). Infrared, Convective, and Sequential  
541 Infrared and Convective Drying of Wine Grape Pomace. *Drying Technology*, 32 (6),  
542 686-694. doi:[10.1080/07373937.2013.853670](https://doi.org/10.1080/07373937.2013.853670)
- 543 Sukrasno, S., Fidrianny, I., Anggadiredja, K., Handayani, W., & Anam, K. (2011). Influence  
544 of Drying Method on Flavonoid Content of *Cosmos caudatus* (Kunth) Leaves.  
545 *Research Journal of Medicinal Plants*, 5, 189-195. doi:[10.3923/rjmp.2011.189.195](https://doi.org/10.3923/rjmp.2011.189.195)
- 546 Sun, J., Zhang, X., Qiu, X., Zhu, X., Zhang, T., Yang, J.,... Wang, H. (2020). Hyperspectral  
547 data for predicting moisture content and distribution in scallops during continuous and  
548 intermittent drying. *Drying Technology*, 1-14. doi:[10.1080/07373937.2020.1837153](https://doi.org/10.1080/07373937.2020.1837153)
- 549 Téllez-Pérez, C., Mounir, S., Montejano, J. G., Sobolik, V., Anaberta, C.-M., & Allaf, K.  
550 (2012). Impact of Instant Controlled Pressure Drop Treatment on Dehydration and  
551 Rehydration Kinetics of Green Moroccan Pepper (*Capsicum Annuum*). *procedia*  
552 *Engineering*, 42. doi:[10.1016/j.proeng.2012.07.491](https://doi.org/10.1016/j.proeng.2012.07.491)

- 553 Tetang Fokone, A., Marcel, E., & Alexis, K. (2020). Intermittent Drying of Mango Slices  
554 (Mangifera indica L.) "Amelie": A New Model. American Journal of Food Science and  
555 Technology, 8, 81-86. doi:10.12691/ajfst-8-3-1
- 556 Tiho, T., Yao, J. C. N. g., Brou, C. Y., & Adima, A. A. (2017). Drying Temperature Effect on  
557 Total Phenols and Flavonoids Content, and Antioxidant Activity of Borassus  
558 aethiopum Mart Ripe Fruits' Pulp. Journal of Food Research, 6 (2), 50.  
559 doi:10.5539/jfr.v6n2p50
- 560 Umesh Hebbar, H., & Rastogi, N. K. (2001). Mass transfer during infrared drying of cashew  
561 kernel. Journal of Food Engineering, 47 (1), 1-5. doi:https://doi.org/10.1016/S0260-  
562 8774 (00)00088-1
- 563 Vega-Galvez, A., Zura-Bravo, L., Lemus-Mondaca, R., Martinez-Monzo, J., Quispe-Fuentes,  
564 I., Puente, L., & Di Scala, K. (2015). Influence of drying temperature on dietary fibre,  
565 rehydration properties, texture and microstructure of Cape gooseberry (*Physalis*  
566 *peruviana* L.). J Food Sci Technol, 52 (4), 2304-2311. doi:10.1007/s13197-013-1235-0
- 567 Vishwanathan, K. H., Hebbar, H. U., & Raghavarao, K. S. M. S. (2010). Hot Air Assisted  
568 Infrared Drying of Vegetables and Its Quality. Food Science and Technology Research,  
569 16 (5), 381-388. doi:10.3136/fstr.16.381
- 570 Wanyo, P., Siriamornpun, S., & Meeso, N. (2011). Improvement of quality and antioxidant  
571 properties of dried mulberry leaves with combined far-infrared radiation and air  
572 convection in Thai tea process. Food and Bioproducts Processing, 89 (1), 22-30.  
573 doi:10.1016/j.fbp.2010.03.005
- 574 Yang, Z., Zhu, E., Zhu, Z., Wang, J., & Li, S. (2013). A comparative study on intermittent heat  
575 pump drying process of Chinese cabbage (*Brassica campestris* L.ssp) seeds. Food and  
576 Bioproducts Processing, 91 (4), 381-388. doi:10.1016/j.fbp.2013.02.006

577 Zaccari, F., & Galietta, G. (2015). alpha-Carotene and beta-Carotene Content in Raw and  
578 Cooked Pulp of Three Mature Stage Winter Squash "Type Butternut". *Foods*, 4 (3),  
579 477-486. doi:10.3390/foods4030477

580

581 **FIGURE CAPTIONS**

582 Figure 1: Schematic representation of the laboratory infrared prototype dryer: 1- Fan, 2-  
583 Infrared lamps, 3- Sample, 4- Dryer Chamber, 5- Power control.

584 Figure 2: Schematic diagram of water transfer and vapor transport mechanisms during IIRAD.

585 Figure 3: Effect of drying mode and parameters on kinetics versus the effective drying time.

586 Figure 4: Evolution of Evaporating bulb temperature versus time for different drying modes;  
587 (continuous, Type I-IIRAD, and Type II-IIRAD)

588 Figure 5: Evolution of Evaporating-bulb Temperature versus Drying Rate

589 Figure 6: Specific energy consumption during continuous IR drying, IIRAD type I and IIRAD  
590 type II of squash, compared with (\*) results of conventional infrared drying of potatoes  
591 (Hebbar et al., 2004).

592 Figure 7: Rehydration rate for continuous IR and IIRAD dried squash

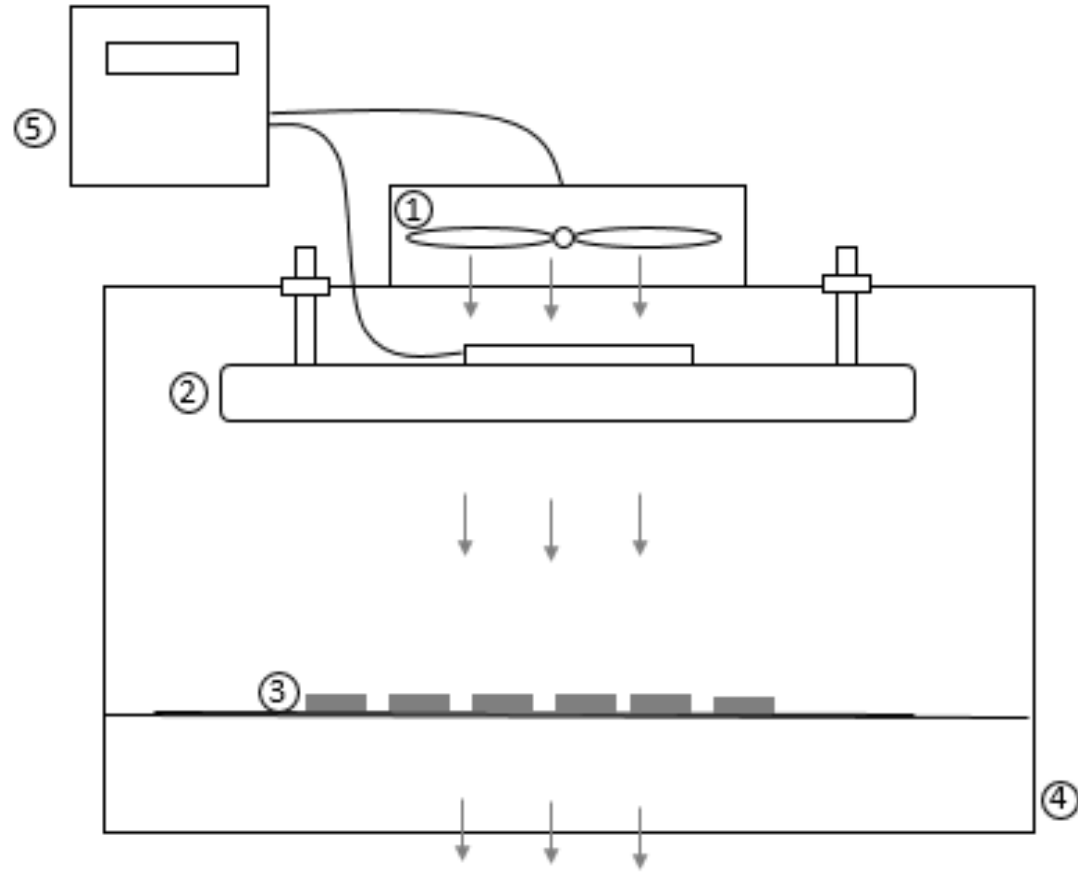


**Fig 1.** Schematic representation of the laboratory infrared prototype dryer: 1- Fan, 2- Infrared lamps, 3- Sample, 4- Dryer Chamber, 5- Power control.

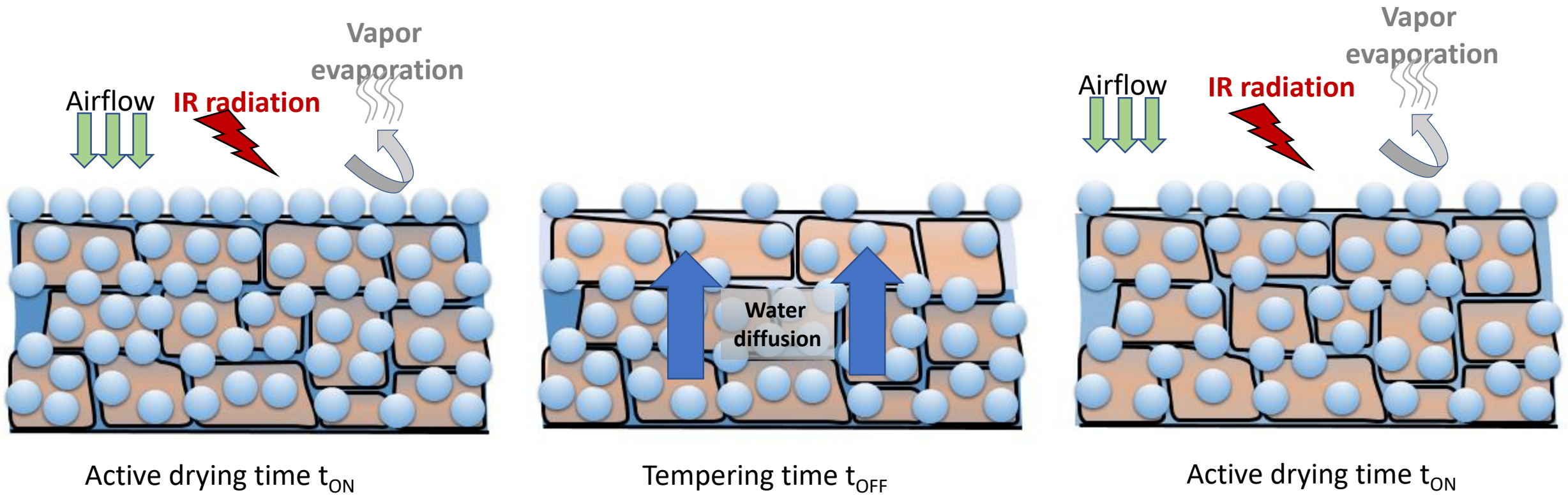


**Fig. 2.** Schematic diagram of water transfer and vapor transport mechanisms during IIRAD

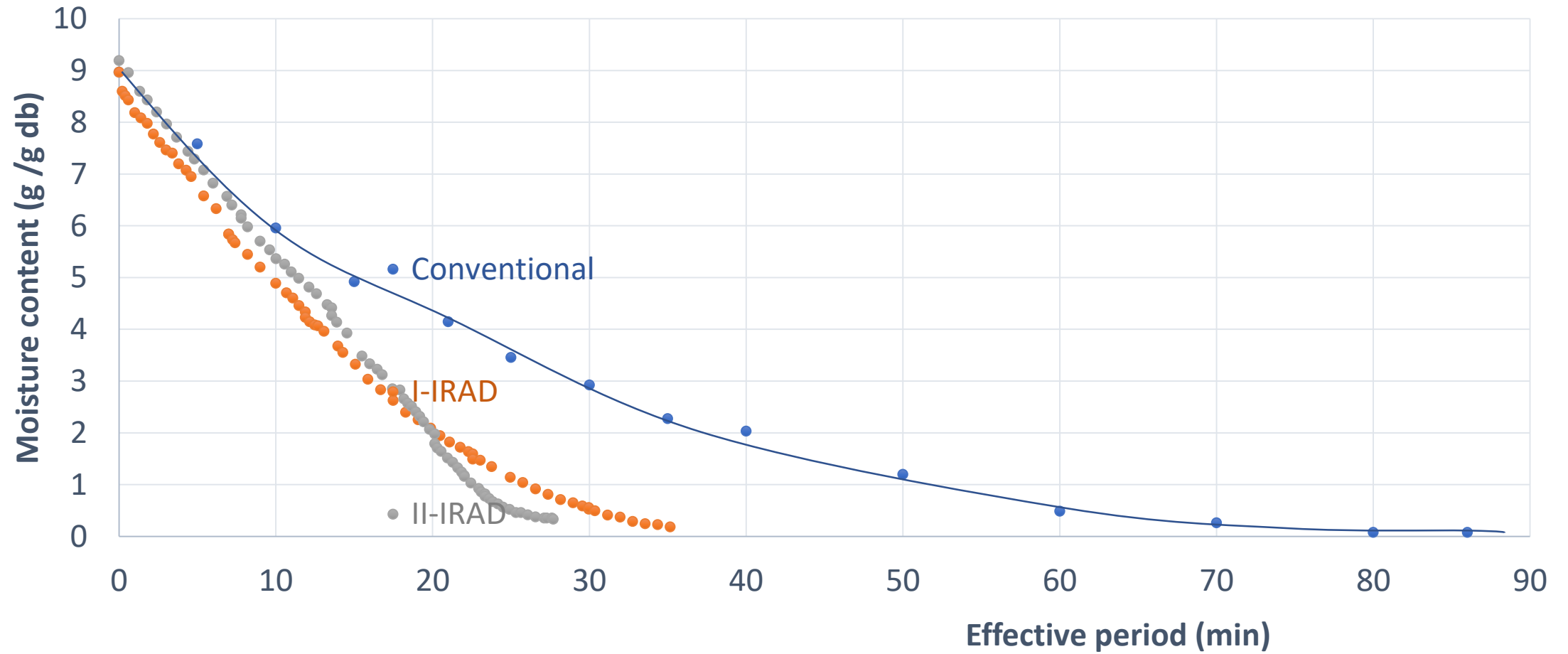


Fig. 3. Effect of drying mode and parameters on kinetics versus the effective drying time.

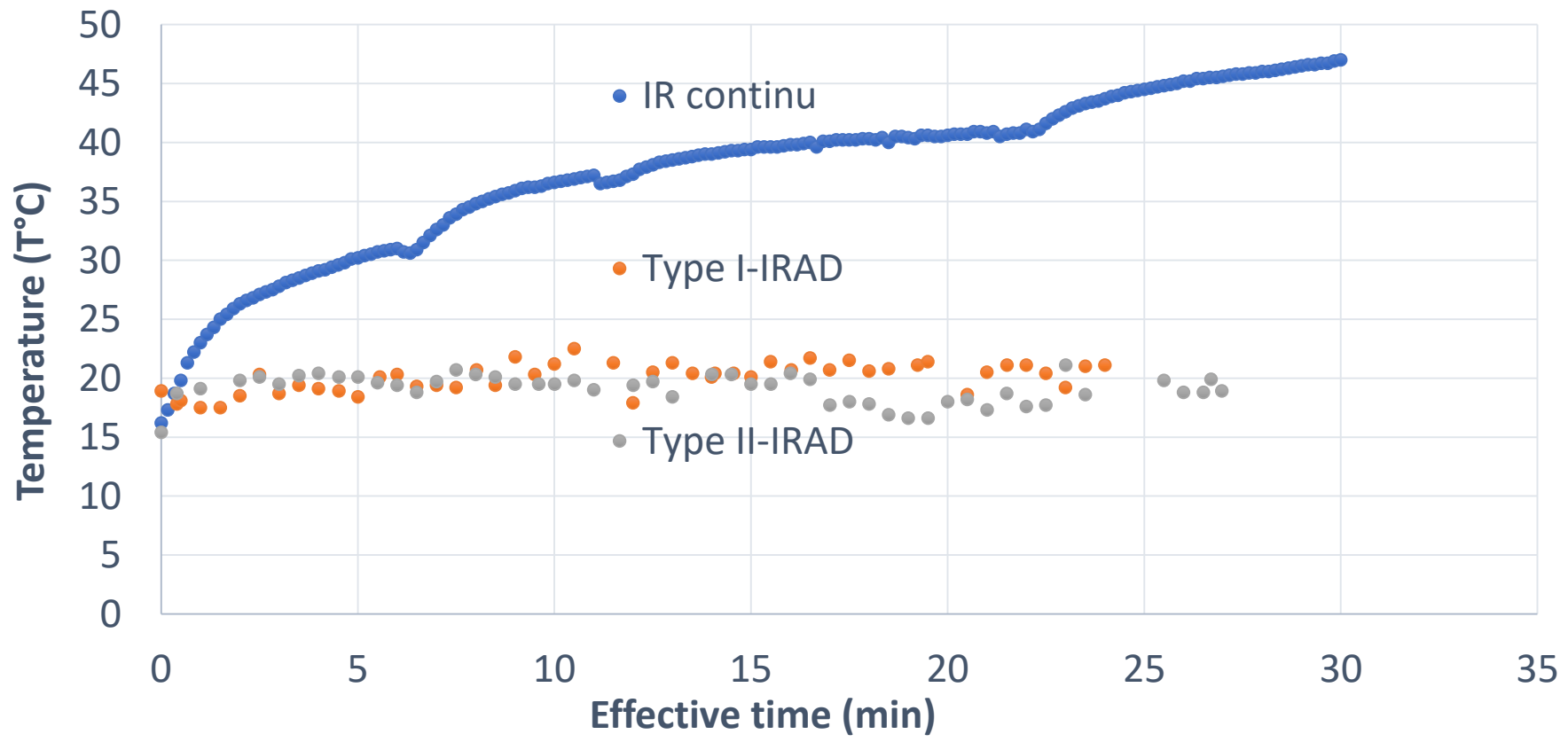


Fig. 4. Evolution of Evaporating bulb temperature during versus time for different drying modes; (continuous, Type I-IIRAD, and Type II-IIRAD).

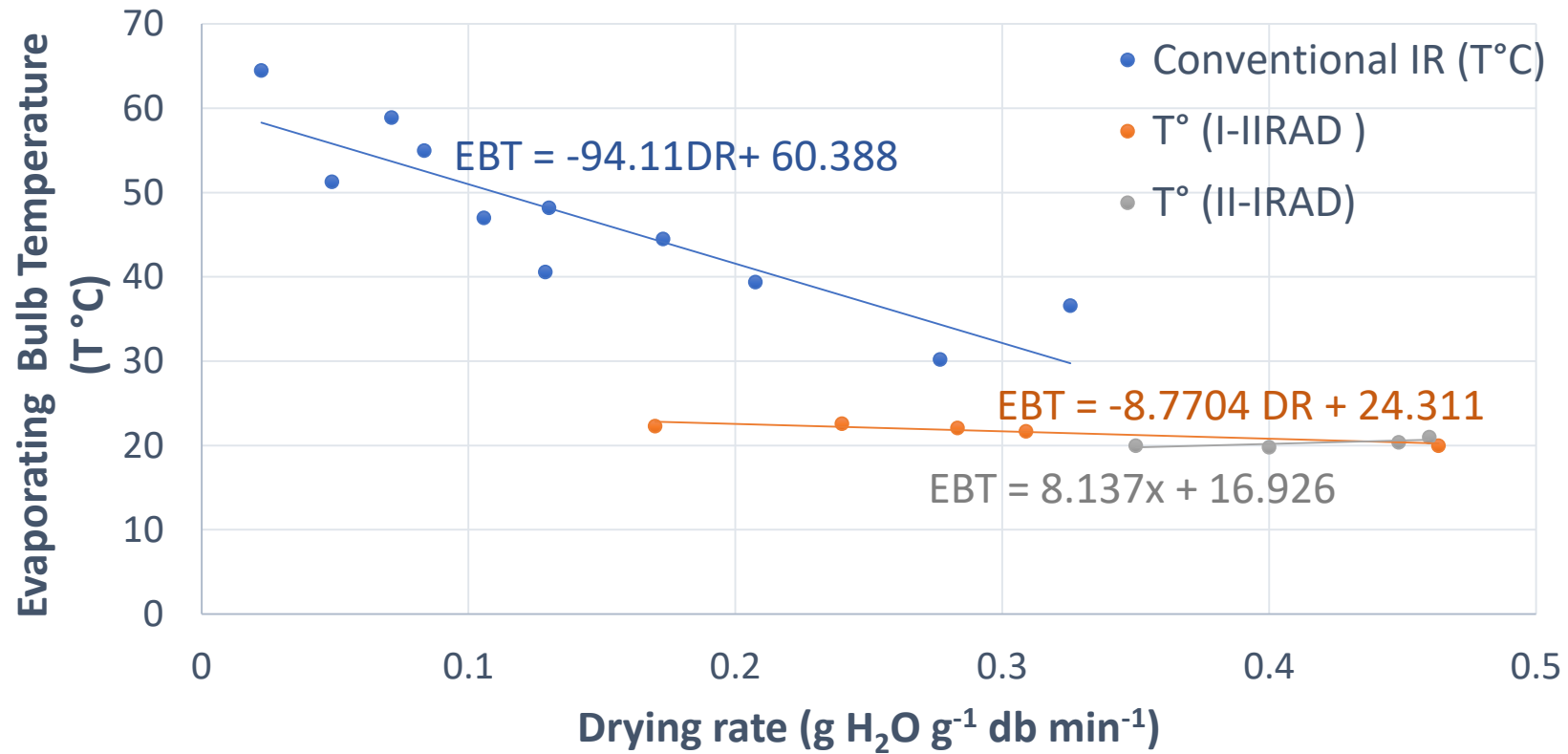


Fig. 5. Evolution of Evaporating-Bulb Temperature (EBT) versus Drying Rate (DR).

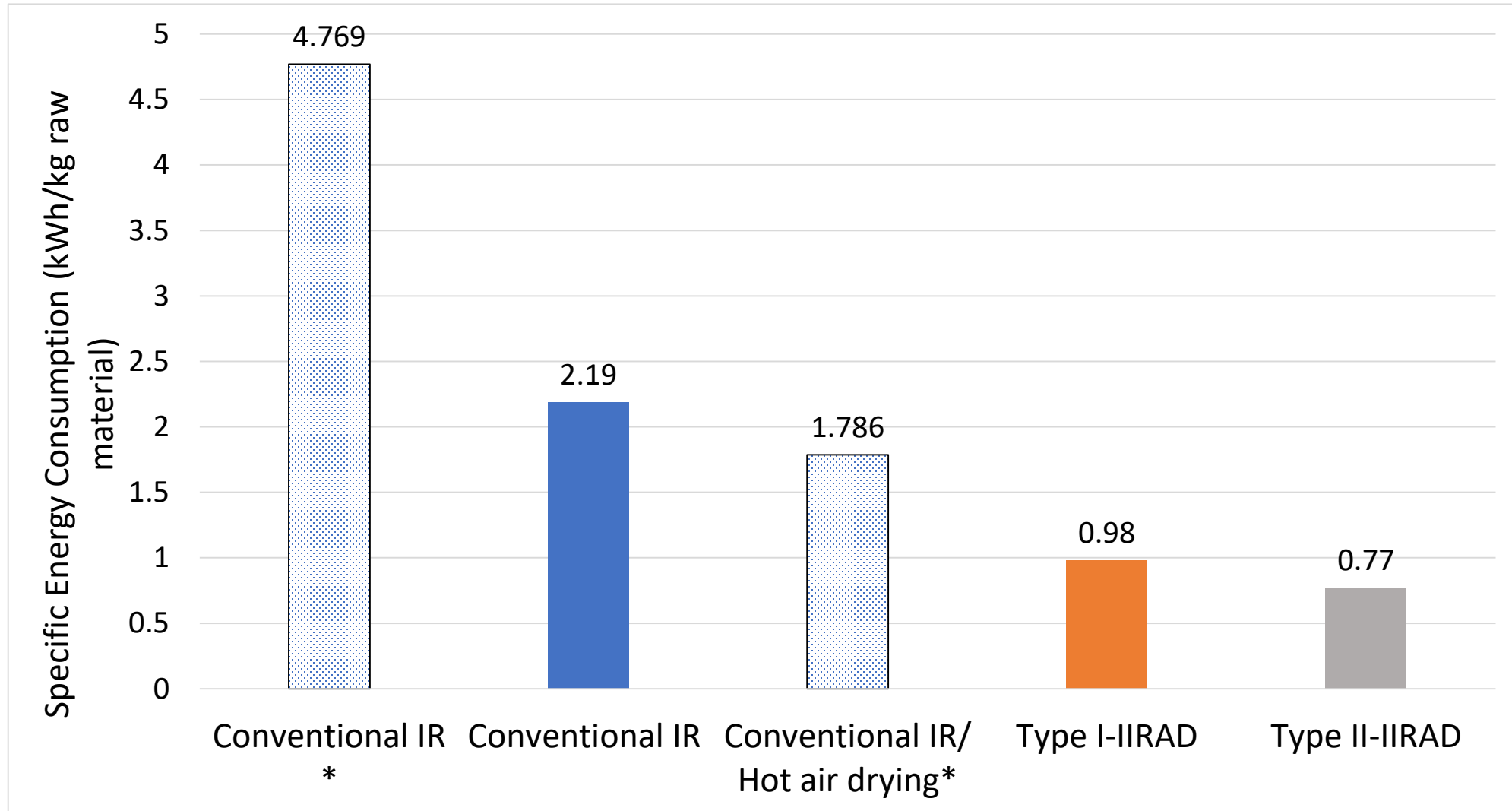


Fig.6. Specific energy consumption during continuous IR drying, IIRAD type I and IIRAD type II of squash, compared with (\*) results of conventional infrared drying of potatoes (Hebbar et al., 2004).

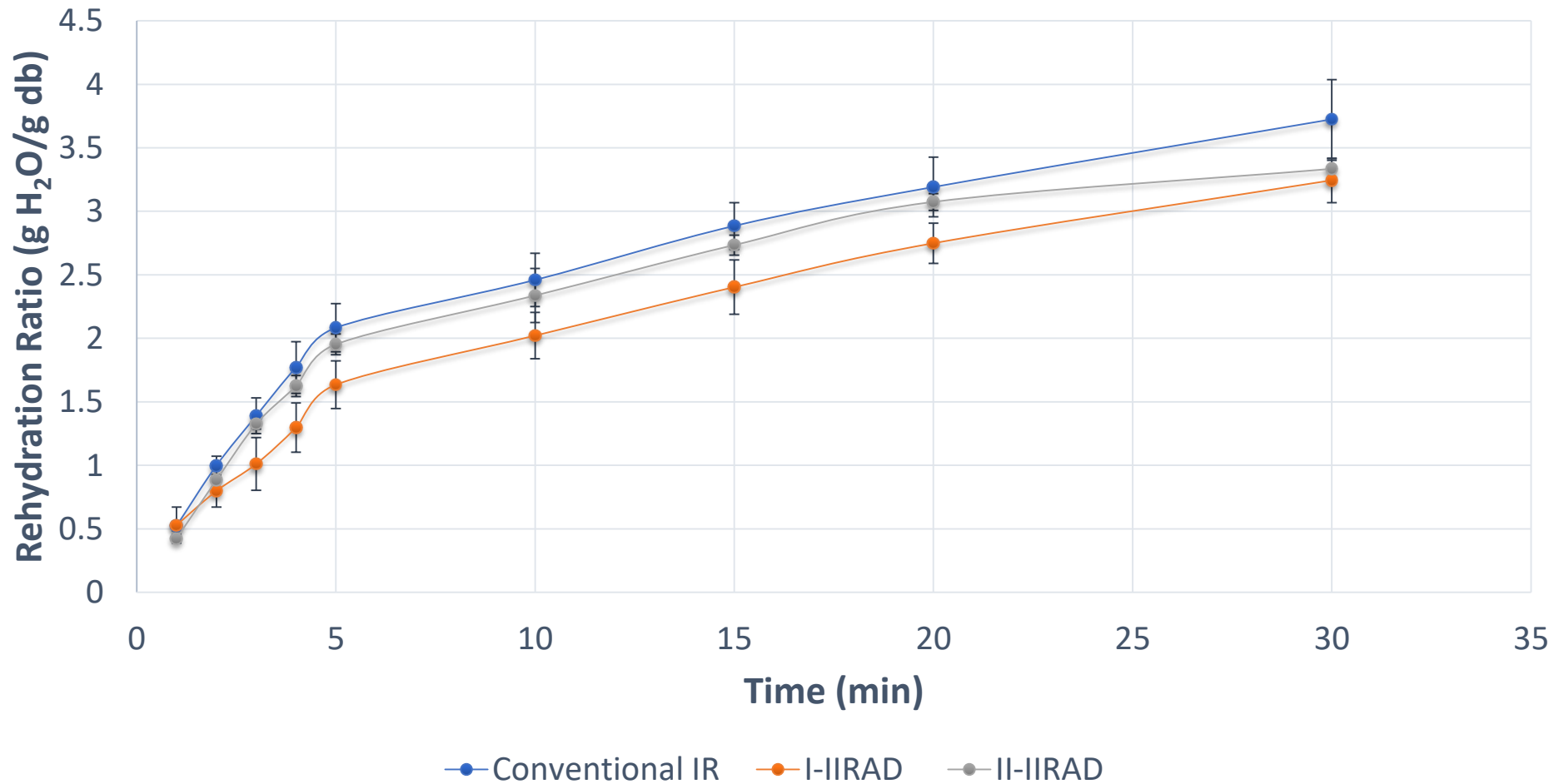


Fig. 7. Rehydration rate for continuous and IIRAD dried squash.

Table 1. IR energy consumption with 0.7 W/cm<sup>2</sup> IR source, an exchange surface of 10 cm<sup>2</sup>, the total mass of material of 4.82 ± 0.07g, and the water weight of 4.23 ± 0.09g.

Drying processes	∑Active Drying Time	IR Specific Energy (Eq. 1)	Total IR Energy	$m_v$	Specific Energy consumption (Eq. 3)	
	min	(J/cm <sup>2</sup> )	(J)	(g)	(kJ/g H <sub>2</sub> O)	(kWh/kg H <sub>2</sub> O)
<b>IR continue</b>	80	3360	33600	4,3 <sup>a</sup> ±0.1	7.877 <sup>a</sup> ±0.18	2.19 <sup>a</sup> ±0.05
<b>Type I-IIRAD</b>	35	1470	14700	4.19 <sup>a</sup> ±0.1	3.51 <sup>b</sup> ±0.09	0.97 <sup>b</sup> ±0.03
<b>Type II-IIRAD</b>	28	1176	11760	4.24 <sup>a</sup> ±0.08	2.77 <sup>c</sup> ±0.05	0.77 <sup>c</sup> ±0.02

Notes: Values are given as mean ± standard deviation (SD) of three independent tests. Different letters in the same row indicate significantly different values (p < 0.05)

Table 2. Quality parameters of dried pumpkin at different IR drying mode.

<b>Variable</b>	<b>Continuous</b>	<b>Type I-IIRAD</b>	<b>Type II-IIRAD</b>
Final Moisture content (g H <sub>2</sub> O/g db)	0.21 ±0.07	0.27 ±0.028	0.26 ±0.023
L*	84.17 <sup>b</sup> ±0.37	78.02 <sup>a</sup> ±0.27	76.86 <sup>c</sup> ±0.36
a*	4.87 <sup>b</sup> ±0.61	14.2 <sup>c</sup> ±0.57	15.39 <sup>c</sup> ±0.89
b*	7.60 <sup>b</sup> ±0.39	17.93 <sup>c</sup> ±0.25	18.22 <sup>c</sup> ±0.86
ΔE	20.77 <sup>a</sup> ±0.61	9.42 <sup>b</sup> ±0.20	9.66 <sup>b</sup> ±0.64
TPC loss (%)	42.70 <sup>a</sup> ±2.75	47.18 <sup>b</sup> ±2.98	48.42 <sup>b</sup> ±0.91
Flavonoid loss (%)	68.08 <sup>a</sup> ± 1.08	51.63 <sup>b</sup> ± 1.24	64.10 <sup>c</sup> ± 2.15

Notes: Values are given as mean ± standard deviation (SD) of three independent tests.

Different letters in the same row indicate significantly different values (p < 0.05)